

# Analytical Study on Roll-Up Method for Deployable Membrane

Masaya Kurakawa<sup>(1)</sup>, Nobukatsu Okuizumi, Osamu Mori, Yasutaka Sato<sup>(2)</sup>,  
Yasuyuki Miyazaki<sup>(3)</sup>, Hiraku Sakamoto<sup>(4)</sup>, Yoshiki Sugawara<sup>(1)</sup>, Kazuya Saito<sup>(5)</sup>

<sup>(1)</sup>Department of Mechanical Engineering, Aoyama Gakuin University

<sup>(2)</sup>Institute of Space and Aeronautical Science, Japan Aerospace Exploration Agency

<sup>(3)</sup>Department of Aerospace Engineering, Nihon University

<sup>(4)</sup>Department of Mechanical Engineering, School of Engineering, Tokyo Institute of Technology

<sup>(5)</sup>Department of Mechanical and Biofunctional Systems, Institute of Industrial Science, The University of Tokyo

## Abstract

In recent years, a large space membrane structure attracts attention and various storage methods have been studied. The difference in circumferential length that occurs when rolling-up and storing a folded membrane structure has been improved by contrivance of folding such as forming a crease of a curved line, but it is difficult to manufacture on a large membrane used in space is there. Therefore, there has been proposed a rolling-up method in which the membrane on which the crease of the straight line is formed is slacked at regular intervals, and the difference in circumferential length is locally reduced to zero. Until now, experiments have succeeded in rolling-up with suppressed formation of new fold lines and demonstrated effectiveness. However, because the tension during rolling-up was not controlled, the thickness of rolling-up was uneven. In addition, a dynamic model considering stiffness of membrane and tension has not yet been constructed. In this research, we aim to derive a dynamic model and clarify deformation characteristics by the above method.

## 展開膜面における巻き付け方法の解析的研究

倉川 正也<sup>(1)</sup>, 奥泉信克, 森 治, 佐藤泰貴<sup>(2)</sup>, 宮崎康行<sup>(3)</sup>, 坂本啓<sup>(4)</sup>, 菅原 佳城<sup>(1)</sup>, 斎藤一哉<sup>(5)</sup>

<sup>(1)</sup>青山学院大学

<sup>(2)</sup>宇宙航空研究開発機構(JAXA), 宇宙科学研究所(ISAS)

<sup>(3)</sup>日本大学,

<sup>(4)</sup>東京工業大学

<sup>(5)</sup>東京大学

## 摘要

近年、大型の宇宙膜面構造物が注目されており、様々な収納方法が検討されてきた。折り畳まれた膜構造物を巻付け収納する際に生じる周長差はこれまで曲線の折り目を形成する等の折り畳みの工夫により改善されてきたが、宇宙で用いられる大型膜面では製作が困難である。そこで、直線の折り目を形成した膜面を一定間隔で弛ませ、局所的に周長差をゼロとする巻付け手法が提案されている。これまで、実験により、新たな折線の形成を抑えた巻付けに成功し、有効性が示されたが、巻付け時の張力が管理されなかった事で、巻付け厚さに不均一を引起こした。加えて、膜剛性や張力を考慮した力学的なモデルは未だ構築されていない。本研究では力学モデルを導出し、上記手法での変形特性を解明する事を目的とする。

## 1. Introduction

### 1.1 Background

In recent years, a large membrane structure having a thickness of several micro and a shape of several to several tens of meter attracts attention, and various storage methods have been studied<sup>(1)-(2)</sup>. As an example, there is the IKAROS<sup>(3)</sup> solar power sail demonstration spacecraft launched by JAXA in 2010. In IKAROS, a huge membrane with a thickness of 7.5  $\mu\text{m}$  and a size of 14  $\times$  14 m was folded and wrapped around the side of the cylindrical body by Z-folding. Considering the thickness

of film when rolling up a cylindrical shape here, there is a problem that circumferential difference occurs inside and outside the folded membrane. However, in IKAROS, inner and outer circumference differences did not matter.

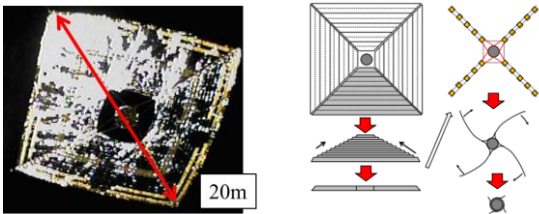


Fig. 1.1. IKAROS and how to fold of IKAROS by Z-folding.

Currently JAXA is considering the plan of "OKEANOS<sup>(4)</sup>" next-generation solar power sail spacecraft in the 2020s. Compared to IKAROS, this probe has a larger membrane size, the number of Z-folded and the number of devices to be mounted are very large, so it is impossible to ignore the difference in inner and outer circumferences when rolling-up the membrane. As a result, the position of the polygonal line is stored in a state deviated. In order to solve this problem, by managing the phase by predicting the inner and outer circumference differences arising from the membrane and the thickness of device, and further by the mechanism that does not propagate the wave shape generated by the inner and outer circumference difference to the leading end side, a method of eliminating the circumferential difference has been proposed (Fig.2).

## 1.2 PREVIOUS RESEARCH

Up to now, the rolling-up experiment<sup>(5)-(8)</sup> under conditions close to the actual machine was performed, and it was confirmed that reproducible rolling-up with suppressed generation of new fold lines is possible. On the other hand, it is not possible to predict the rolling-up thickness beforehand because  $\psi$  in figure 1.2 does not become constant interval due to the rolling-up phase, and as a result of creating Wave shape, its slack causes unevenness in circumferential thickness. The problem was pointed out. Also, studies on this rolling-up method have been limited to simple geometric models so far, and a model considering the rigidity of the membrane and the tension at the time of rolling-up has not yet been constructed. Furthermore, actual size rolling-up test requires a lot of manpower from film production to rolling-up test, modeling in wave shape rolling-up to know the thickness of rolling-up beforehand from the viewpoint of the spacecraft design is urgent.

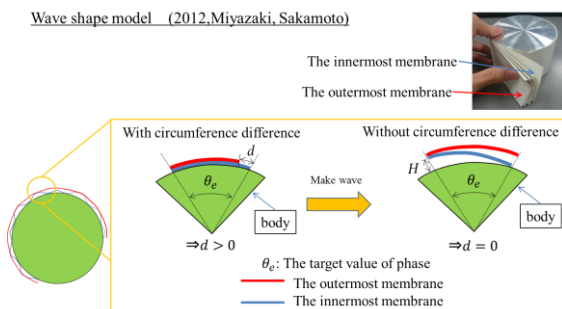


Fig. 1.2. Method of roll-up by wave shape.

In this research, we aim to deepen the understanding of the mechanical properties at the time of rolling-up of Z-folded membrane structure. Specifically, the following two points are summarized.

- Model the membrane structure when it is wrapped in Wave shape and verify the validity of the analysis model by comparing it with the experiment.
- Confirm the possibility of realization of Wave shape rolling-up after managing the tension which has not been considered in the conventional model.

## 2. Modeling in rolling-up process of multilayer folded membrane structure

### 2.1 Brazier effect

Figure 2.1 shows the innermost layer and the outermost layer of the Z-folded membrane structure wound by wave shape. In this study, we apply a previous study of Brazier<sup>(9)</sup> and model it at the time of winding a cross section of a Z-folded membrane structure, and when the wave shape repeats at a constant angle of rolling-up  $\psi$  at the radius of center hub  $r$  is analyzed.

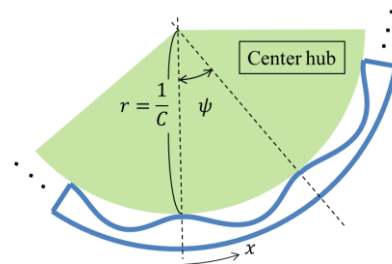


Fig. 2.1. Rolling-up model.

As shown in figures 2.2 and 2.3, the cross section is flattened as the curvature increases when the thin circular tube is bent. As the cross section becomes flattened and becomes an ellipse, the second moment of area decreases and the flexural rigidity decreases. This effect is called the Brazier effect, and Brazier derived the relational expression of bending moment and curvature to the above phenomenon.

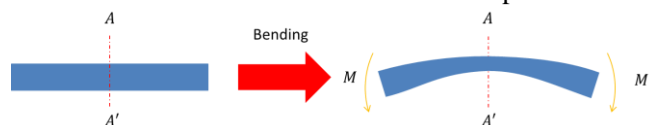


Fig. 2.2. Tube used for Brazier effect.

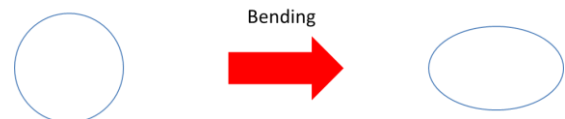


Fig. 2.3. Cross-section of tube used for Brazier effect.

As a preliminary step due to deformation of the circular tube, as shown in figure 2.1, the tendency due to bending of the two elastically connected beams was investigated. It is assumed that the beam before deformation is linear and stress is not applied to the whole. When a uniform bending moment is applied, one

beam is tensioned and the other beam is compressed. Since the beam deforms according to Hooke's law, we assume that the plane part of the beam is perpendicular to the bent axis. At this time, since it is performed symmetrically for stable and uniform bending, the deformed shape has a uniform curvature with respect to the beam. Thus, the two beams are curved members in tension and compression, respectively, and the spring is in a compressed state. As these springs become infinitely stiff, their lengths do not change, there is no change in the cross-sectional dimensions of the beams, which is a classical equation for the bending of the elastic beam as shown in equation (2.1). On the other hand, if these springs are relatively soft, the distance between the beams decreases, increasing the curvature for the beam for a given bending moment. At this time, the entire buckling of the beam is caused by the bending, but the local buckling that partially buckles does not occur. The spring occupying the unit length of the original shape of the beam has a spring constant  $k_b$  and these are assumed to be uniformly distributed along the length of the beam.

Below the beam receives deformation by bending and compression, so we derive the strain energy of each term from the following. Here, the bending moment  $M_b$ , the distance  $H_b$  between the beams, the strain  $\zeta_b$  of the spring due to bending, the cross-sectional area of the beam before deformation has  $A_b$  and the Young's modulus is  $E_b$ .

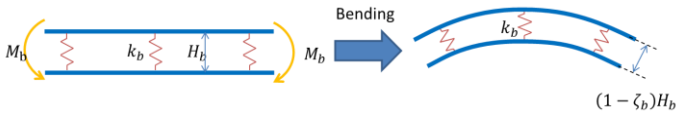


Fig. 2.4. Two beam used for Brazier effect.

Using the flexural rigidity  $E_b I_b$  and the curvature  $C_b$ , the equation by the net bending of the beam can be expressed by the following equation.

$$M_b = C_b E_b I_b \quad (2.1)$$

Here,  $I_b$  is the geometrical moment of inertia about the center of gravity axis.

$$I_b = \frac{1}{4} A_b H_b^2 (1 - \zeta_b)^2 \quad (2.2)$$

The distortion energy  $U^b_{bend}$  due to the bending of the beam per unit length can be expressed as follows.

$$\begin{aligned} U^b_{bend} &= \frac{1}{2} M_b C_b = \frac{1}{2} C_b^2 E_b I_b (\zeta_b) \\ &= \frac{1}{8} C_b^2 E_b A_b H_b^2 (1 - \zeta_b)^2 \end{aligned} \quad (2.3)$$

The distortion energy  $U^b_{comp}$  due to compression of the spring per unit length can be expressed as follows.

$$U^b_{comp} = \frac{1}{2} k_b \zeta_b^2 H_b^2 \quad (2.4)$$

Since the total potential energy  $U^b$  can be represented by the sum of the respective strain energies

minus the work by external force ( $W = 0$ )

$$\begin{aligned} U^b &= U^b_{bend} + U^b_{comp} - W \\ &= \frac{1}{8} C_b^2 E_b A_b H_b^2 (1 - \zeta_b)^2 \\ &\quad + \frac{1}{2} k_b \zeta_b^2 H_b^2 \end{aligned} \quad (2.5)$$

Here, the displacement in rolling-up is the curvature  $C_b$  by bending and the strain  $\zeta_b$  of the spring. Therefore, according to the principle of minimum potential energy, the following two equations hold in order to minimize  $U^b$  at a position where the gradient of the function  $U^b$  of total strain energy becomes 0, that is, when the partial differential regarding a certain parameter becomes 0.

$$\frac{\partial U^b}{\partial \zeta_b} = -\frac{1}{4} C_b^2 E_b A_b (1 - \zeta_b) + k_b \zeta_b = 0 \quad (2.6)$$

$$\begin{aligned} \frac{\partial U^b}{\partial C_b} &= \frac{1}{4} C_b^2 E_b A_b H_b^2 (1 - \zeta_b)^2 + k_b \zeta_b^2 H_b \\ &= 0 \end{aligned} \quad (2.7)$$

From equation (3.6),  $\zeta_b$  can be expressed as follows.

$$\zeta_b = \frac{c^2}{1 + c^2} = \frac{\frac{1}{4} C_b^2 \frac{A_b E_b}{k_b}}{1 + \frac{1}{4} C_b^2 \frac{A_b E_b}{k_b}} \quad (2.8)$$

As shown figure 2.1, in this theory, it is assumed that the occurring wave shape is a repeating structure as shown in the figure, and one element is analyzed as shown in figure 2.5. One element is the belly part of the cross section, that is, the layer thickness is from the thickest position to the next thickest position. Here,  $x$  is the object coordinate of the membrane element,  $\psi$  is the angle of rolling-up of the membrane element, that is, the angle at which wave shape occurs, and  $H_b$  is the layer thickness when wave shape is rolling up.

The spring constant  $k$  in this study is modeled as the crease rigidity of the Z-folded membrane structure.

Also, as described above, the spring constants of the two elastically connected beams are all equal, and since the entire beam is bent, the two beams have the same shape. Therefore, in order to model the distortion  $\zeta$  of the spring due to bending in this research, it is necessary to change the location of the spring and change it according to the position of the center hub. Therefore, in order to give periodicity to the placement position of the spring, we introduce a function such as equation (2.9) where  $\zeta = 0$  for  $x = 0$ ,  $r\psi$  and  $\zeta x = r\psi/2$ , maximizing modeling in this study.

$$\begin{aligned} \zeta &= \frac{c^2}{1 + c^2} \sin^2 \left( \frac{\pi x}{r\psi} \right) \\ &= \frac{C^2 AE}{4k + C^2 AE} \sin^2 \left( \frac{\pi x}{r\psi} \right) \\ &= \frac{X_2 C^2}{X_1 + X_2 C^2} \sin^2 \frac{X_3}{\psi} x \end{aligned} \quad (2.9)$$

where  $X_1 = 4k$ ,  $X_2 = AE$ ,  $X_3 = \frac{\pi}{r}$ .

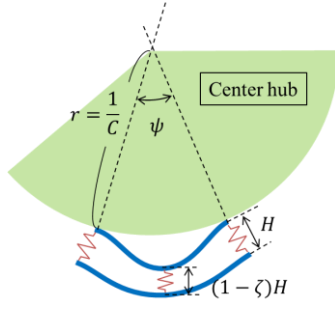


Fig. 2.5. A figure focusing on one element of Fig. 2.1.

We derive the strain energy according to each deformation mode as in the formulation in the previous section.

$$\begin{aligned}
 U_{bend} &= \int_0^L \frac{1}{2} C^2 EI(\zeta) dx \\
 &= \int_0^L \frac{1}{8} C^2 EA H^2 (1 - \zeta)^2 dx \\
 &= \frac{1}{8} C^2 X_2 H^2 \int_0^L \left( 1 - 2 \frac{X_2 C^2}{X_1 + X_2 C^2} \sin^2 \frac{X_3}{\psi} x + \left( \frac{X_2 C^2}{X_1 + X_2 C^2} \sin^2 \frac{X_3}{\psi} x \right)^2 \right) dx \\
 &= \frac{1}{8} C^2 X_2 H^2 L \left( 1 - \frac{X_3}{\psi} X_5 + \frac{3X_3}{8\psi} X_5^2 \right) \\
 &= \frac{1}{8} C^2 X_2 H^2 r \psi \left( 1 - X_6 X_5 \left( \frac{8}{3} - X_5 \right) \right)
 \end{aligned} \tag{2.10}$$

The strain energy due to spring compression can be expressed as follows.

$$\begin{aligned}
 U_{compress} &= \int_0^L \int_0^{\zeta H} \frac{1}{2} k \zeta H dz dx \\
 &= \int_0^L \frac{1}{2} k \zeta^2 H^2 dx \\
 &= \int_0^L \frac{1}{2} k H^2 \left( \frac{X_2 C^2}{X_1 + X_2 C^2} \sin^2 \frac{X_3}{\psi} x \right)^2 dx \\
 &= \frac{1}{2} k H^2 X_5^2 \frac{3X_3}{8\psi} L = \frac{1}{2} k H^2 X_5^2 X_6 r \psi
 \end{aligned} \tag{2.11}$$

where  $X_4 = X_1 + X_2 C^2$ ,  $X_5 = \frac{X_2 C^2}{X_4}$ ,  $X_6 = \frac{3X_3}{8\psi}$ .

Here, work  $W$  due to external force is thought to be caused by the tension loaded on the membrane element as shown in figure 2.6, so it can be expressed by the following equation(2.12).

$$\begin{aligned}
 W &= T \sin \psi (r - r \cos \psi) + T \cos \psi (r \sin \psi - r \psi) \\
 &= r T \sin \psi - r \psi T \cos \psi \\
 &= \frac{T}{C} (\sin \psi - \psi \cos \psi)
 \end{aligned} \tag{2.12}$$

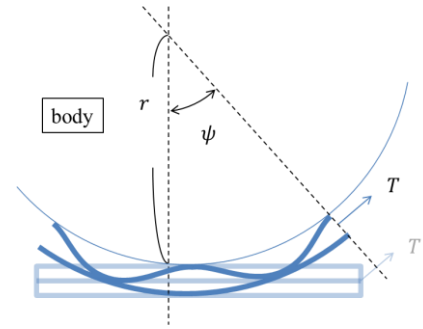


Fig. 2.7. Work by external force.

Therefore, the total potential energy can be expressed as follows.

$$\begin{aligned}
 U &= U_{bend} + U_{comp} - W \\
 &= \frac{1}{8} C^2 X_2 H^2 r \psi \left( 1 - \frac{8}{3} X_6 X_5 + X_6 X_5^2 \right) \\
 &\quad + \frac{1}{2} k H^2 X_5^2 X_6 r \psi \\
 &\quad - \frac{T}{C} (\sin \psi - \psi \cos \psi)
 \end{aligned} \tag{2.13}$$

Equations (2.14) and (2.15) are obtained from the principle of minimum potential energy as in the previous section.

$$\begin{aligned}
 \frac{\partial U}{\partial C} &= \frac{\partial U_{bend}}{\partial C} + \frac{\partial U_{comp}}{\partial C} - \frac{\partial W}{\partial C} = 0 \\
 \Leftrightarrow X_7 \left[ \left( \frac{2}{C} + 1 \right) - \frac{8}{3} X_6 X_8 (1 + X_9) + X_6 X_8^2 (1 + 2X_9) \right] \\
 &\quad + \frac{8X_6 X_7 X_8 k}{X_4} + \frac{T}{C^2} (\sin \psi - \psi \cos \psi) = 0
 \end{aligned} \tag{2.14}$$

$$\begin{aligned}
 \frac{\partial U}{\partial \zeta} &= \frac{\partial U_{bend}}{\partial \zeta} + \frac{\partial U_{comp}}{\partial \zeta} - \frac{\partial W}{\partial \zeta} = 0 \\
 \Leftrightarrow \frac{X_7}{\psi} - \frac{1}{4} k H^2 X_6 X_8^2 C^2 r + \frac{T}{C} \psi \sin \psi = 0
 \end{aligned} \tag{2.15}$$

where  $X_7 = \frac{1}{8} C^2 X_2 H^2 r \psi$ ,  $X_8 = \frac{2X_2 C}{X_4}$ ,  $X_9 = \frac{X_1}{X_5}$ .

These two equations are the governing equations in the rolling-up. By simultaneous establishment of these two equations, two unknowns  $\psi$ ,  $H$ , three unknowns, are determined. On the other hand, the spring constant  $k$  is obtained by an experiment.

### 3. Results of analysis

Table 2.1 shows the parameters for performing the analysis in this section. This is actually a material parameter similar to that used in the solar power sail OKEANOS.

Table 2.1 Parameter.

Fixed parameters	
Young's modulus $E$ [GPa]	4.1 GPa
Thickness $t$ [m]	10e-6 m
Width of folding $d$ [m]	30e-3 m
Radius of center hub $r$ [mm]	150

### 3.1 Relation between tension $T$ and height of wave shape $H$

First, in order to confirm the tendency of the analysis result, we analyzed the tension in a wide range of orders. Figure 3.1-3.3 shows the tension  $T$  - height of wave shape  $H$  graph when the radius is fixed, in which the spring constant  $k$  is changed in order. As an example, the result when the spring constant is  $k = 10 \text{ N / m}$  is shown. As a result, as the overall tendency, the height of wave shape is smaller with increasing tension, which shows that it agrees with the physical tendency. On the other hand, there was no significant change depending on the spring constant.

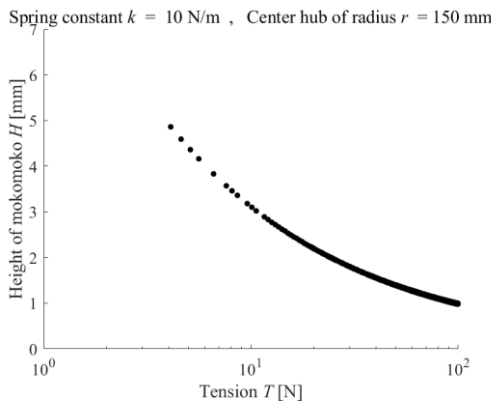


Fig. 3.1.  $T$ - $H$  graph at  $k = 10 \text{ N/m}$ .

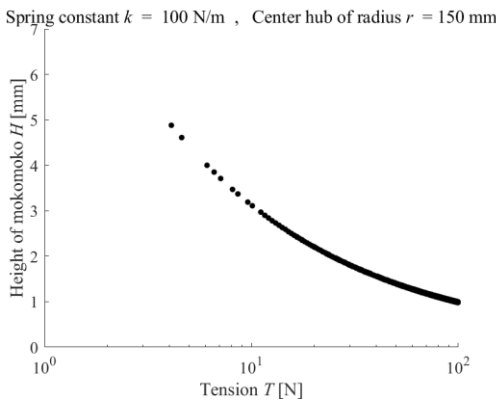


Fig. 3.2.  $T$ - $H$  graph at  $k = 100 \text{ N/m}$ .

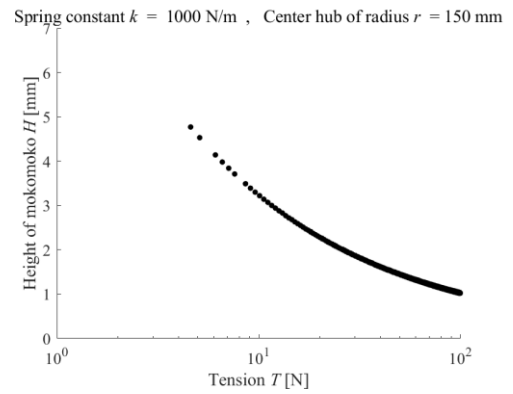


Fig. 3.3.  $T$ - $H$  graph at  $k = 1000 \text{ N/m}$ .

### 3.2 Relationship between tension $T$ and winding angle $\psi$

In order to confirm the trend similarly to the previous section, we analyzed the tension in a wide range of orders. Figure 3.4-3.6 shows the tension  $T$  - angle of rolling-up  $\psi$  graph when the radius is fixed. Hereinafter, as an example, the result when the spring constant is  $k = 10 \text{ N / m}$  is shown. As a result, it can be seen that the winding angle  $\psi$  is constant regardless of the increase of the tension as the overall tendency. On the other hand, there was no significant change depending on the spring constant.

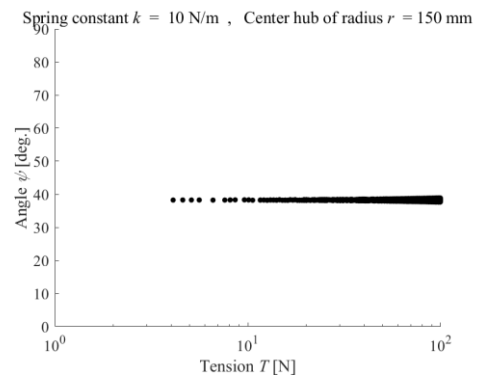


Fig. 3.4.  $T$ - $\psi$  graph at  $k=10 \text{ N/m}$

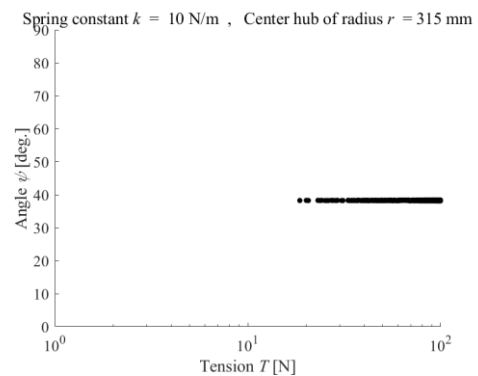


Fig. 3.5.  $T$ - $\psi$  graph at  $k=100 \text{ N/m}$

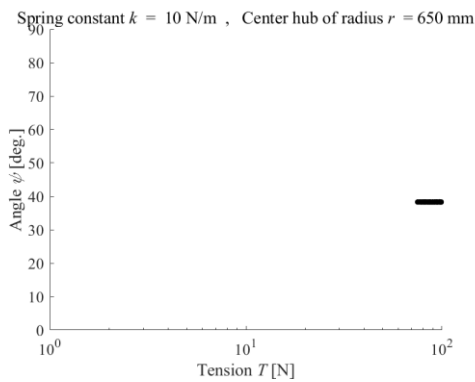


Fig. 3.6.  $T$ - $\psi$  graph at  $k=1000$  N/m.

#### 4. Conclusion · Future tasks

The conclusion in this research is summarized below.

- We modeled method of roll-up by wave shape by Brazier theory.
- Analysis results show that the height of wave shape decreases due to the increase in tension. In addition, it was found that the angle of rolling-up is constant regardless of the tension. It was confirmed that the value of the spring constant does not greatly affect the result in this analysis.

In the future, we plan to carry out the experiment, verify the validity of the model, and improve the analytical model considering the change of wave shape depending on the material.

#### Reference

- (1) Guest, S. D., and S. Pellegrino. "A new concept for solid surface deployable antennas." *Acta Astronautica* Vol. 38.2, 1996, pp. 103-113.
- (2) T.Nojima, "Modeling of a thin cylindrical membrane folding method considering easy deployment by origami", papers of the Japan Society of Mechanical Engineers (Part C), Vol. 67, No. 653, 2001, pp. 270-275.
- (3) O.Mori, Y.Tsuda, H.Sawada, T.Sayuki, R.Funase, "IKAROS Technology (Solar Sail)", *Journal of Artificial Intelligence Society*, Vol.26, No.2, 2011, pp. 164-175.
- (4) O. Mori et al: "Jovian Trojan Asteroid Exploration by Solar Power Sail-craft", *Transactions of the Japan Society for Aeronautical and Space Sciences, Aerospace Technology Japan*, Vol. 14, No.30, pp 1-7, 2016 .
- (5) N.Okuizumi et al, "Study on large solar power sail membrane deployment structure / mechanism for Jupiter Trojan cluster exploration", *Proceedings of 15th Space Science Symposium (2015)*, <https://repository.exst.jaxa.jp/dspace/bitstream/a-is/549157/1/SA6000034259.pdf> [Access date: 2018, 10, 15].
- (6) Y.Shirasawa et al., "Development of large sail membrane surface of solar power sail and consideration of storage and deployment method", *Proceedings of 13th Space Science Symposium (2013)*, <http://www.isas.jaxa.jp/j/researchers/symp/sss13/paper/P2-128.pdf> [Access date: 2018, 10, 31]
- (7) SAITO, Kazuya, et al. "Experimental Research on Roll-up Storage Method for a Large Solar Sail", In *4th International Symposium on Solar Sailing 2017*, pp. 1-5.
- (8) S.Kadanishi, "Research on the storage method of solar sails considering the thickness of members", master thesis, Tokyo Institute of Technology, 2012.
- (9) C. R. CALLADINE, "THEORY OF SHELL STRUCTURES", CAMBRIDGE UNIVERSITY PRESS, 1983, pp. 595 - 604